



Contents lists available at SciVerse ScienceDirect

Magnetic Resonance Imaging



Measuring small compartments with relatively weak gradients by angular double-pulsed-field-gradient NMR

Darya Morozov^a, Leah Bar^b, Nir Sochen^b, Yoram Cohen^{a,*}

^a School of Chemistry, Sackler Faculty of Exact Sciences, Tel Aviv University, Ramat Aviv, Tel Aviv 69978, Israel

^b School of Mathematical Sciences, The Raymond and Beverly Sackler Faculty of Exact Science, Tel Aviv University, Tel Aviv, Israel

ARTICLE INFO

Article history:

Received 5 August 2012

Accepted 31 August 2012

Available online xxx

Keywords:

NMR Spectroscopy

Diffusion NMR

Double-Pulsed-Field-Gradient (d-PFG)

Bipolar Gradients

Microstructure

Compartment Size

ABSTRACT

NMR diffusion–diffraction patterns observed in compartments in which restricted diffusion occurs are a useful tool for direct extraction of compartment sizes. Such diffusion–diffraction patterns may be observed when the signal intensity $E_{(q,\Delta)}$ is plotted against the wave-vector \mathbf{q} (when $\mathbf{q} = (2\pi)^{-1}\gamma\delta\mathbf{G}$). However, the smaller the compartment sizes are, the higher are the q -values needed to observe such diffractions. Moreover, these q -values should be achieved using short gradient pulses requiring extremely strong gradient systems. The angular double-pulsed-field gradient (d-PFG) NMR methodology has been proposed as a tool to extract compartment sizes using relatively low q -values. In this study, we have used single-PFG (s-PFG) NMR and angular d-PFG NMR to characterize the size of microcapillaries of about $2 \pm 1 \mu\text{m}$ in diameter. We found that these microcapillaries are characterized by relatively strong background gradients that completely masked the effects of the microscopic anisotropy (μA) of the sample, resulting in a completely unexpected $E(\varphi)$ profile in the angular d-PFG NMR experiments. We also show that bipolar angular d-PFG NMR experiments can largely suppress the effect of these background gradients resulting in the expected $E(\varphi)$ profile from which the compartment dimensions could be obtained with relatively weak gradient pulses. These results demonstrate that the above methodology provides a quick, reliable, non-invasive means for estimating small pore sizes with relatively weak gradients in the presence of large magnetic susceptibility.

© 2012 Published by Elsevier Inc.

1. Introduction

Non-invasive measurement of small size compartments is of great importance in a myriad of chemical and biological applications [1–3]. The pulsed-gradient spin-echo (PGSE) NMR experiment, which was introduced by Stejskal and Tanner in 1965 [4], is indeed the most widely used method for measuring diffusion [1–6], and for extracting micro-structural information non-invasively in systems such as porous materials [1,2,7–9], emulsions [10], rocks [11–13], cells [14,15] and neuronal tissues [3]. Diffusion NMR was also used to study organometallic complexes [16], supramolecular system [17], nanoparticles [18] and nanotubes [19].

It is well known that free diffusion is Gaussian and that there the signal decay can be analyzed using the well-known Stejskal–Tanner equation from which the diffusion coefficient can be extracted. In free diffusion the root mean square displacement (rmsd) increases with the square root of the diffusion time (\sqrt{t}). In restricted compartments that are mono-disperse in size, when the signal intensity ($E(\mathbf{q})$) in the single-pulsed-field-gradient (s-PFG) NMR experiment is plotted as a function of the wave-vector \mathbf{q} (when $\mathbf{q} = (2\pi)^{-1}\gamma\delta\mathbf{G}$), where γ is the magnetic gyro ratio, δ and \mathbf{G} are the pulse gradient duration and

intensity, respectively), diffusion–diffraction minima should be and are observed experimentally [20,21]. It was shown that from such diffusion–diffractions the compartment size can be extracted directly for simple known geometries [22]. However, these diffusion–diffraction minima may easily disappear as a result of size poly-dispersity [23] or because of susceptibility effects induced by the inhomogeneity of the sample [23]. The use of bipolar (bp) gradient pulses [24,25] in such NMR experiments can recover the diffusion–diffractions minima in inhomogeneous samples and may allow extracting the relevant microstructural information, but only in systems that are mono-disperse in size [26].

Many chemical and biological systems are characterized by size poly-dispersity where diffusion–diffraction minima are generally not observed when s-PFG NMR experiments are performed. In such cases the way to extract the compartment size is by Fourier transformation of the signal decay ($E(\mathbf{q})$). The methodology was originally developed by Cory and Garroway [27]. There the compartment size can, in principle, be estimated from full-width at half-height (FWHH) or from the base of the displacement probability distribution profile [28–32]. Extraction of the correct displacement distribution profile in a system with restricted diffusion is possible under the long diffusion time scale and short gradient pulse (SGP) approximation [20,21].

Another way to extract the compartment size in systems which are characterized by size poly-dispersity is by using the double-PFG (d-

* Corresponding author. Tel.: +972 3 6407232; fax: +972 3 6407469.

E-mail address: ycohen@post.tau.ac.il (Y. Cohen).

PFG) NMR experiment. The d-PFG NMR experiment was first proposed by Cory et al. in 1990 [33]. The d-PFG NMR sequence employs two diffusion sensitizing gradient pairs, G_1 and G_2 , with duration δ_1 and δ_1 , respectively, that are separated by a mixing time t_m . The two gradient pairs may be applied collinearly or with an angle between them yielding the radial and angular d-PFG NMR experiments, respectively [33,34]. Two diffusion time intervals, Δ_1 and Δ_2 , exist in these sequences. Both theoretical and experimental studies of the signal decay in d-PFG experiments performed on systems exhibiting restricted diffusion demonstrated that zero-crossings of the signal that are analogous to the diffusion-diffraction minima in s-PFG experiments should be and are observed in such NMR experiments [35,36]. In addition, these zero-crossings were very recently found to be more robust toward poly-dispersity in sizes [23].

To characterize compartments with an inner diameter of about $2\mu\text{m}$ (comparable to the diameter of axons in WM) using the diffusion-diffractions or the zero-crossings observed in the single or double PFG MR experiments, respectively, would necessitate reaching q-values of more than 6100cm^{-1} . To fulfill the SGP approximation,

extremely strong gradients of more than 1400G/cm in the s-PFG experiment should be used assuming δ is set to 1 ms. Gradient systems capable of producing only up to less than 100G/cm are now common on small animal MRI scanners and those of clinical scanners are capable of producing only $5\text{--}8\text{G/cm}$ because of safety issues and technological limitations. Thus a possible means for measuring small compartments of about $2\mu\text{m}$ with common gradient systems seems to be the use of the angular d-PFG NMR methodology introduced by Mitra [34,37–39]. Indeed, in recent years, angular d-PFG NMR is attracting much attention [37–47].

In the present study we challenged the ability of single-PFG and double-PFG NMR experiments to probe the compartment sizes as small as $2\mu\text{m}$. Both single- and angular double-PFG NMR experiments and their bipolar versions were used to characterize non-invasively the inner diameter of such microcapillaries where the ground truth is known a priori. The data from all NMR experiments were fitted to the appropriate cylindrical model. We found that the bipolar (bp) angular d-PFG NMR experiments can characterize such systems which are also characterized by relatively large magnetic inhomogeneity.

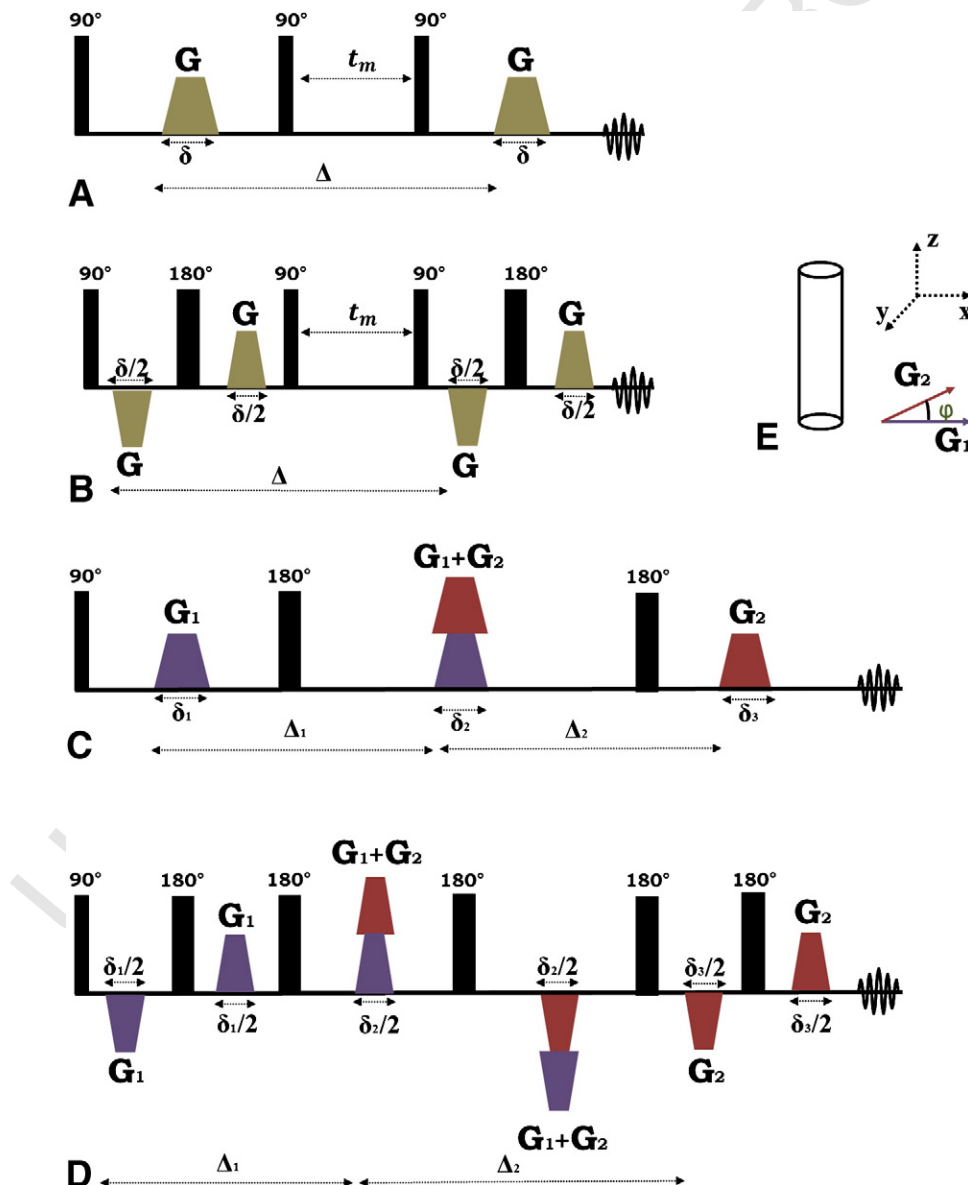


Fig. 1. Single-pulsed-gradient stimulated echo (s-PGSTE) with (A) monopolar and (B) bipolar gradients. The double-pulsed-gradient spin echo (d-PGSE) sequences with $t_m=0$ with (C) monopolar and (D) bipolar gradients. (E) The angular d-PFG is performed by setting $|G_1|=|G_2|$ and by varying only the angle φ between the two gradient pairs.

126 **2. Experimental methods**

127 **2.1. General**

128 The NMR experiments were performed on a Bruker 8.4T NMR
 129 spectrometer capable of producing up to 190G/cm along each of the
 130 three directions. Microcapillaries with a known inner diameter of $2 \pm$
 131 $1\mu\text{m}$ and outer diameter of $150 \pm 1\mu\text{m}$ (Polymicro Technologies,
 132 Phoenix, AZ, USA) were cut to micro-tubes of about 3 cm in length and
 133 dipped in water for a week, prior to each experiment. The
 134 microcapillaries were then packed into a glass sleeve (8mm) and
 135 inserted into a 10mm NMR tube. The NMR tube was aligned parallel
 136 to the z direction of the magnet.

137 **2.2. NMR experiments**

138 The s-PFG and d-PFG NMR experiments were first performed
 139 using conventional monopolar gradients, and then the experiments
 140 were repeated using bipolar gradients. The gradients in the
 141 monopolar sequences are characterized by their duration δ and
 142 amplitude G . To reach the same q value in the bipolar sequences,
 143 the gradient amplitude G was kept the same as in the monopolar
 144 version, and the gradient pulse duration was split into two parts
 145 with duration $\delta/2$, and a π pulse was symmetrically placed between
 146 the two gradient pulses.

147 The single-pulsed-gradient stimulated-echo (s-PGSTE) and the
 148 bp-s-PGSTE NMR experiments shown in Fig. 1A and B, respective-
 149 ly, were performed in the x-direction with the following
 150 parameters: 40 q values were collected with $G_{max} = 160\text{G/cm}$,
 151 $\delta = 4\text{ms}$, resulting in a maximal q value of 2724cm^{-1} , Δ was set
 152 to 30 ms.

153 The angular double-pulsed-gradient spin-echo d-PGSE and the bp-
 154 d-PGSE NMR experiments shown in Fig. 1C and D, respectively, were
 155 performed in the x-y plane in which G_1 was fixed along the x-axis and
 156 the orientation of G_2 was varied. The measurements were conducted for
 157 25 different values of φ between 0 and 360, 8 q values were collected
 158 with $G_{max} = 80\text{G/cm}$, $t_m = 0\text{ms}$, $\delta_1 = \delta_2 = \delta_3 = 4\text{ms}$, $\Delta_1 = \Delta_2 =$
 159 30ms , resulting in a $q_{max} = 1362\text{cm}^{-1}$ for both experiments. The
 160 fitting of the angular bp-d-PGSE NMR was performed according to
 161 references [38] and [39]. Note that this fitting takes into consider-
 162 ation the finite values of δ . The fitting of the s-PFG was performed as
 163 described below.

164 **2.3. s-PFG data fittings**

165 Let $E_s(q)$ denote the theoretical magnetization in an s-PFG
 166 sequence and $E_d(q)$ the theoretical magnetization in a d-PFG sequence
 167 according to Eq. (21) in reference [42]. Specifically,

$$E_d(\mathbf{q}_1, \mathbf{q}_2, r_0) = [\exp\{-\Lambda\delta_1 + i2\pi\mathbf{q}_1 \cdot \mathbf{A}\} \exp\{-\Lambda(\Delta_1 - \delta_1)\} \\ \times \exp\{-\Lambda\delta_1 - i2\pi\mathbf{q}_1 \cdot \mathbf{A}\} \exp\{-\Lambda(t_m - \delta_1)\} \\ \times \exp\{-\Lambda\delta_2 - i2\pi\mathbf{q}_2 \cdot \mathbf{A}\} \exp\{-\Lambda(\Delta_2 - \delta_2)\} \\ \exp\{-\Lambda\delta_2 - i2\pi\mathbf{q}_2 \cdot \mathbf{A}\}]_{0,0},$$

169 and
 170

$$E_s(\mathbf{q}, r_0) = [\exp\{-\Lambda\delta + i2\pi\mathbf{q} \cdot \mathbf{A}\} \exp\{-\Lambda(\Delta - \delta)\} \exp\{-\Lambda\delta - i2\pi\mathbf{q} \cdot \mathbf{A}\}]_{0,0},$$

172 where the multiplications of the exponentials result in a matrix and
 173 we only take its (0,0) element. The matrices Λ and \mathbf{A} depend on the
 174 geometry of the compartment.
 175

In the case of microcapillaries which correspond to an infinite
 cylinder geometry with radius r_0 and diffusion coefficient d_0 [39],

$$\Lambda_{km,k'm'}(r_0) = \delta_{kk'}\delta_{mm'} \frac{\alpha_{km}^2 D_0}{r_0^2}$$

$$\mathbf{A} = \begin{pmatrix} X \\ Y \end{pmatrix},$$

where

$$X_{km,k'm'}(r_0) = r_0 \delta_{m,m' \pm 1} \sqrt{1 + \delta_{m,0} + \delta_{m',0}} \beta_{km} \beta_{k'm'} \frac{\alpha_{km}^2 + \alpha_{k'm'}^2 - 2mm'}{(\alpha_{km}^2 - \alpha_{k'm'}^2)^2}$$

$$Y_{km,k'm'}(r_0) = ir_0 (\delta_{m,m' + 1} - \delta_{m,m' - 1}) \\ \times \sqrt{1 + \delta_{m,0} + \delta_{m',0}} \beta_{km} \beta_{k'm'} \frac{\alpha_{km}^2 + \alpha_{k'm'}^2 - 2mm'}{(\alpha_{km}^2 - \alpha_{k'm'}^2)^2},$$

$\delta_{mm'}$ stands for the Kronecker delta, and α_{km} is the k^{th} zero of the
 derivative of the m^{th} Bessel function satisfying $J'_m(\alpha_{km}) = 0$.

Finally

$$\beta_{km} = \begin{cases} 1 & k = m = 0 \\ \frac{\alpha_{km}}{\sqrt{\alpha_{km}^2 - m^2}} & \text{otherwise} \end{cases}.$$

We denote the measured magnetization as $M_s(\mathbf{q})$ and $M_d(\mathbf{q})$ for
 the single and double sequences respectively. The estimation of the
 microstructure radius r_0 is performed by minimizing the mean least
 square error,

$$r_0 = \operatorname{argmin}_r \sum_i (E_s(\mathbf{q}_i, r) - M_s(\mathbf{q}_i))^2,$$

or

$$r_0 = \operatorname{argmin}_r \sum_i (E_d(\mathbf{q}_1 i, \mathbf{q}_2 i, r) - M_d(\mathbf{q}_1 i, \mathbf{q}_2 i))^2.$$

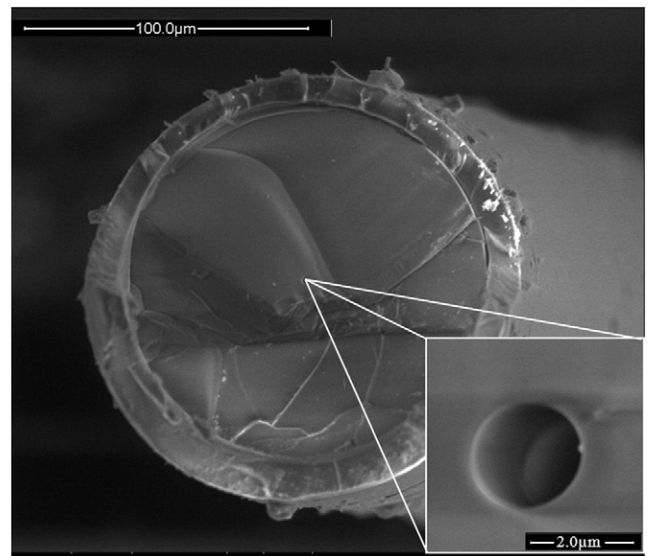


Fig. 2. The low vacuum scanning electron microscopy (SEM) image of $2 \pm 1\mu\text{m}$ microcapillaries at two different magnifications.

201 The minimization was carried out using the Matlab® (R2008a,
202 MathWorks, MA, USA) library function lsqnonlin.

203 The SEM images were collected on a FEI Quanta 200 field emission
204 gun (FEG) environmental scanning electron microscope (ESEM).

205 3. Results and discussion

206 To validate the accuracy of the microstructural information
207 extracted by different methods, microcapillaries of known diameters
208 should be studied. In such systems the accuracy of the different
209 methods and approaches can be challenged and evaluated. Fig. 2
210 shows the SEM image of such microcapillaries showing that their size
211 is indeed about 2 μm . Clearly, in a sample of an ensemble of such
212 microcapillaries most of the volume is that of the solid materials of the
213 microcapillaries and not of the enclosed liquid in the pores. Therefore

214 both the signal to noise ratio (SNR) and the background gradients can
215 be a problem when studying such systems with NMR.

216 Fig. 3A shows the signal decays of s-PGSTE NMR (black circles) and
217 bp-s-PGSTE NMR (red squares) experiments performed on an
218 ensemble of $2 \pm 1 \mu\text{m}$ microcapillaries in the x-direction with G_{max} of
219 160 G/cm and δ of 4 ms. The signal decay appears larger in the s-PGSTE
220 NMR experiment as compared with the signal decay observed in the
221 bp-s-PGSTE NMR experiment, which corrects for much of the effects of
222 the background magnetic field. However, no diffusion–diffraction
223 minima were observed in these two s-PFG NMR experiments, despite
224 the fact that the microcapillaries are mono-disperse in size and are
225 coherently aligned along the z-direction. It should be noted that such
226 diffusion–diffractions in s-PFG NMR experiments performed on such
227 systems with larger diameters can be easily observed [48]. Fig. 3B
228 shows an attempt to FT the data presented in Fig. 3A. Here, in principle,
229 the mean diameter of the microcapillaries should be extractable from

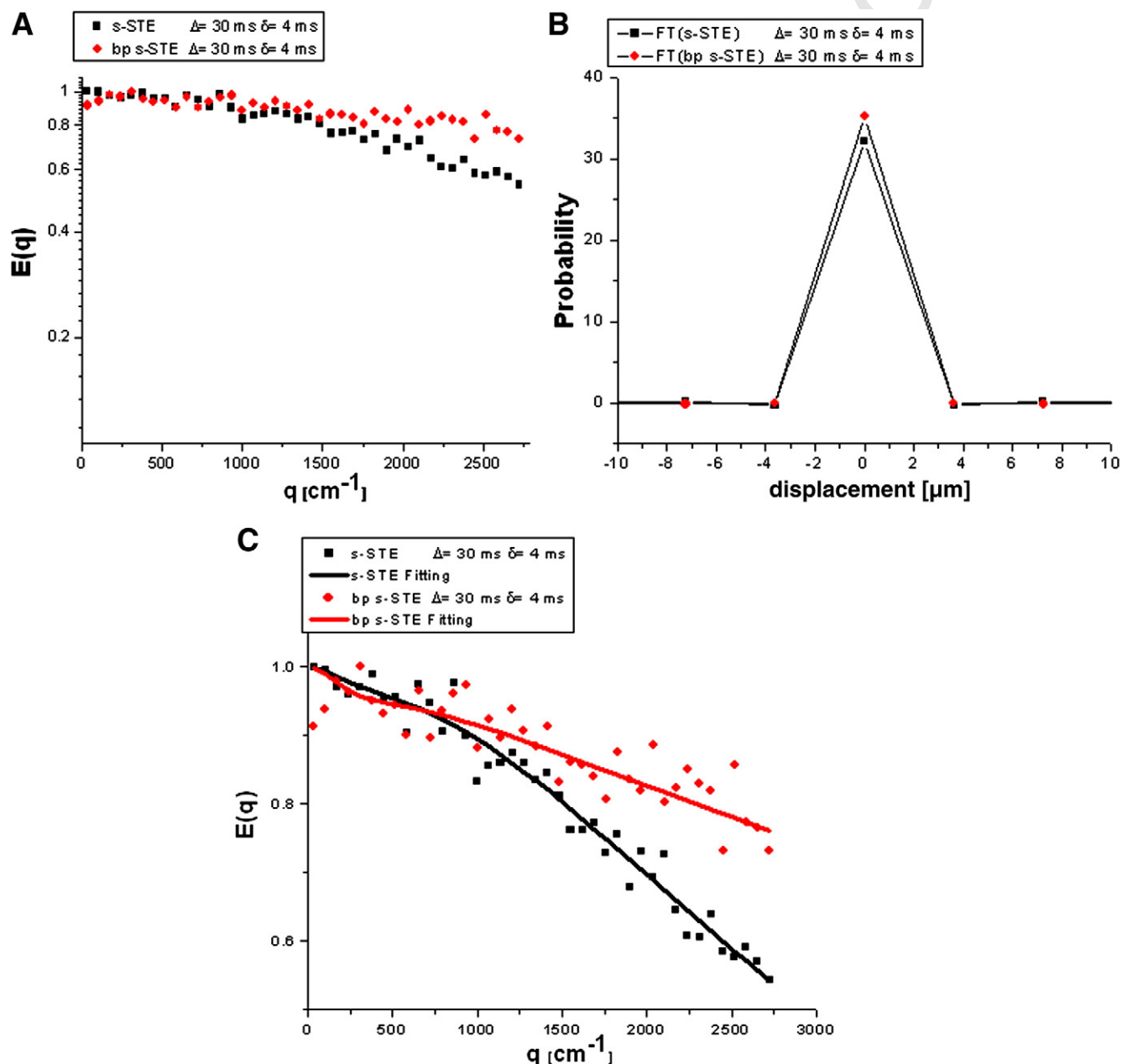


Fig. 3. s-PFG experiments performed on an ensemble of $2 \pm 1 \mu\text{m}$ microcapillaries. (A) The signal decay ($E(q)$) as a function of q -values in a conventional (monopolar) s-PGSTE experiment (black circles) and in a bipolar s-PGSTE experiment (red squares). The two diffusion NMR experiments were performed with the same parameters. (B) Displacement distribution profiles obtained by Fourier transformation of the data shown in (A). (C) s-PFG fittings of the data shown in (A). For the fitting procedure see the experimental section.

the base of the displacement distribution profile, since it describes the maximum available displacement in the sample. Despite the two different decay curves (Fig. 3A) the obtained profiles (Fig. 3B) are similar and the extracted mean diameter for both s-PFG NMR experiments is found to be about $3.6\mu\text{m}$ for the $2\pm 1\mu\text{m}$ capillaries, clearly indicating that there is a problem with such a straightforward analysis of the data. However, when we fitted the data according to the method presented in the experimental section, the mean diameters extracted from s-PGSTE and bp-s-PGSTE experiments were found to be 4.2 ± 0.2 and $2.6\pm 0.3\mu\text{m}$, respectively (Fig. 3C). Clearly the compartment size extracted from fitting the data of the bp-s-PGSTE NMR experiment seems to be adequate.

The results from the angular d-PGSE NMR experiments with q of 1362cm^{-1} are presented in Fig. 4. In such d-PFG NMR experiments with zero mixing time (see Fig. 1D), the angular dependence of the signal i.e. $E(\varphi)$, is predicted to follow a bell-shaped function [34,37–41]. However, completely contrary to theoretical predictions, the results of the d-PGSE experiments presented in Fig. 4A show that $E(\varphi)$ increases up to 90° , then decreases up to 180° . This behavior is nearly mirrored from 180° to 360° . These observations are inconsistent with the expected $E(\varphi)$ profile, when $E(\varphi)$ is governed by microscopic anisotropy (μA) that arises from the boundaries of the restricting compartment [37–45]. We hypothesized that here the effect of μA is completely masked by susceptibility effects, which arise from the relatively strong internal gradients within the sample. It was previously shown that the cross-term induced by background gradients can be effectively suppressed using bipolar pulse gradients [24–26]. Therefore, we repeated the experiments by introducing bipolar pulse gradients to the angular d-PFG NMR sequence with the hope of suppressing these effects.

Fig. 4B shows the results obtained from the bipolar angular d-PFG NMR experiment performed on the same sample with the same parameters as the monopolar angular d-PFG experiment (open red squares). Here the $E(\varphi)$ regains its expected form, showing a bell-shaped dependency implying that the susceptibility effects are significantly suppressed. In this case, a size of $3.07\pm 0.04\mu\text{m}$ was obtained from fitting the signal decay according to the derivation of Özarlan [37–39]. It should be noted that the size extracted from the angular bp d-PFG NMR seems to be somewhat larger than the nominal size and the size seen on the SEM images. The reason is most likely the fact that our bipolar gradients could not completely suppress the

effect of the background gradients. As a result, the $E(\varphi)$ regains its expected form but the obtained size was still somewhat larger than the nominal size of the microcapillaries.

Noninvasive measurement of compartment size in opaque systems is of paramount importance in many fields and the ability of different methods to convey such information should be challenged, first, in systems where the “ground truth” is known. Diffusion–diffractions are indeed an excellent indicator of restricted diffusion and are a useful tool to report on compartment sizes at least for compartments of simple geometries [1,2,20–33,49]. However, for small compartments, such diffusion–diffractions are only observed at very high q -values which can be achieved only with very strong gradient systems which are not available in most laboratories. Indeed for observing even the first diffraction of a compartment of $2\mu\text{m}$, gradient systems capable of producing gradient pulses of more than 1400 Gauss/cm are needed (assuming δ of 1 ms). In addition, such diffusion–diffraction patterns generally disappear with size polydispersity. Here we found that FT of the s-PFG data could not convey a meaningful estimate of the compartment size. However, fitting the data of only the bp-s-PFG NMR experiment assuming a cylindrical shape provides an accurate estimate of the compartment size in this mono-disperse sample.

In the present study we used angular d-PFG NMR [37,40–46] to obtain such information with relatively much weaker gradient pulses of about 80 Gauss/cm. Indeed, in recent years we have seen an increase in the use of angular d-PFG MR to obtain information on the compartment size in different samples, but there, in many studies, the ground truth was hard to estimate [45–47,50,51]. The smallest compartment that was measured using this angular d-PFG NMR methodology in a system in which the ground truth is known was of $5\pm 1\mu\text{m}$ [52]. Clearly pushing the limit toward smaller compartments in the range of two micrometers or less is both important and rather difficult. Here we chose to use even smaller microcapillaries, i.e. microcapillaries having a nominal diameter of only $2\pm 1\mu\text{m}$ which is reminiscent to the diameters of axons in the nervous system [31]. Such microcapillaries allow one to challenge the accuracy of the different methods used. In the present system, we found that bipolar gradients are vital for obtaining the expected signal dependency because of background gradients. Indeed we found that with the correct fitting both the bipolar s-PFG and the bipolar angular d-PFG NMR experiments enable one to extract sizes of about $2\mu\text{m}$ with good accuracy even with relatively weak gradients. Fitting the bipolar s-PFG

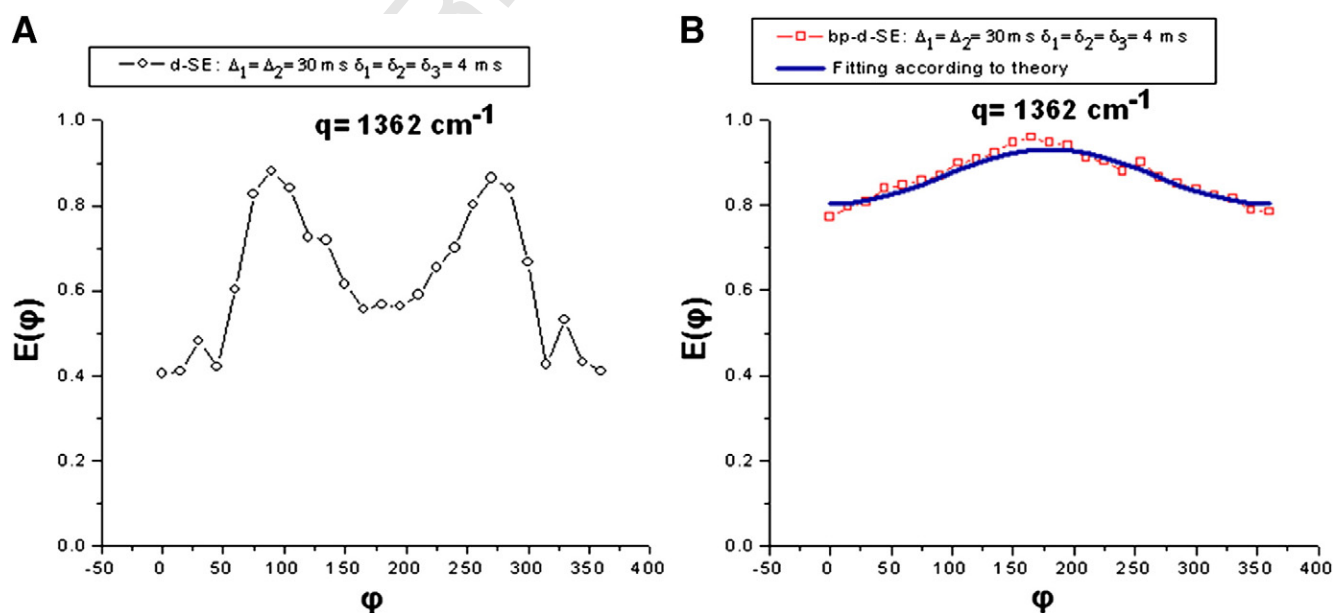


Fig. 4. The $E(\varphi)$ profiles of the angular d-PGSE experiments performed on an ensemble of $2\pm 1\mu\text{m}$ microcapillaries with $q = 1362\text{cm}^{-1}$. (A) Angular d-PGSE with monopolar gradients (open black circles). (B) The $E(\varphi)$ profile of the angular bp-d-PGSE (open red squares) with fitting according to theory in references [38–40] (blue line).

and angular d-PFG NMR data afforded a good estimate of the size of the $2 \pm 1 \mu\text{m}$ microcapillaries.

4. Conclusions

In the present study we challenged the ability of both s-PFG and angular d-PFG NMR methodologies to characterize microcapillaries with an inner diameter of about $2 \pm 1 \mu\text{m}$ with gradient systems of only moderate strength. The diffusion–diffraction minima were not observed in the s-PGSTE NMR experiments performed on these microcapillaries. Trying to obtain an estimation of the compartment dimensions by FT of the signal decay was found to be unreliable. Fitting the bipolar s-PFG NMR data assuming a cylindrical shape allowed for a good estimate of the size of the microcapillaries.

The presence of strong susceptibility effects was also observed in the angular d-PFG experiment resulting in an unexpected $E(\varphi)$ profile. We found that bipolar gradients in the angular bp-d-PFG can suppress most of these effects and the information on the underlying compartment size can be recovered.

These results demonstrate the ability of angular bp-d-PFG NMR experiments to non-invasively measure compartments with size of about $2 \mu\text{m}$ with only moderate gradient systems, even in the presence of significant magnetic inhomogeneity as one should expect to find in porous materials for example.

Acknowledgments

We thank V. Krivitsky and Prof. F. Patolsky from the School of Chemistry of Tel Aviv University for SEM measurements. Partial financial support from the US-Israel Bi-National Foundation (BSF, grant number 2009155) and the CONNECT project administrated by the European Commission under Framework Package 7 is greatly acknowledged.

References


- [1] Callaghan PT. Translational dynamics and magnetic resonance: principles of pulsed gradient spin echo NMR. Oxford: University Press; 2011.
- [2] Price WS. NMR studies of translational motion: principles and applications. Cambridge: University Press; 2009.
- [3] Jones DK, editor. Diffusion MRI: theory, methods and applications. Oxford: University Press; 2011.
- [4] Stejskal EO, Tanner JE. Spin diffusion measurements: spin echoes in the presence of a time-dependent field gradient. *J Chem Phys* 1965;42:288–92.
- [5] Price WS. Pulsed-field gradient nuclear magnetic resonance as a tool for studying translational diffusion I: basic theory. *Concept Magn Reson* 1997;9:299–336.
- [6] Grebenkov DS. NMR survey of reflected Brownian motion. *Rev Mod Phys* 2007;79:1077–137.
- [7] Kukla V, Kornatowski J, Demuth D, Gimus I, Pfeifer H, Rees LVC, et al. NMR studies of single-file diffusion in unidimensional channel zeolites. *Science* 1996;272:702–4.
- [8] Kuntz JF, Trausch G, Palmas P, Mutzenhardt P, Canet DJ. Diffusive–diffraction phenomenon in a porous polymer material observed by NMR using radio-frequency field gradients. *J Chem Phys* 2007;126:134904.
- [9] Song Y-Q, Cho H, Hopper T, Pomerantz AE, Sun PZ. Magnetic resonance in porous media: recent progress. *J Chem Phys* 2008;128(1–12):052212.
- [10] Goudappel GJW, van Duynhoven JPM, Mooren MMW. Measurement of oil droplet size distributions in food oil/water emulsions by time domain pulsed field gradient NMR. *J Colloid Interface Sci* 2001;239:535–42.
- [11] Hurlimann MD, Helmer KG, Latour LL, Sotak CH. Restricted diffusion in sedimentary-rocks — determination of surface-area-to-volume ratio and surface relaxivity. *J Magn Reson A* 1994;111:169–78.
- [12] Song YQ, Ryu SG, Sen PN. Determining multiple length scales in rocks. *Nature* 2000;406:178–81.
- [13] Pape H, Tillich JE, Holz M. Pore geometry of sandstone derived from pulsed field gradient NMR. *J Appl Geophysics* 2006;56:232–52.
- [14] Kuchel PW, Coy A, Stilbs P. NMR “diffusion–diffraction” of water revealing alignment of erythrocytes in a magnetic field and their dimensions and membrane transport characteristics. *Magn Reson Med* 1997;37:637–43.
- [15] Pages G, Yau TW, Kuchel PW. Erythrocyte shape reversion from echinocytes to discocytes: kinetics via fast-measurement NMR diffusion–diffraction. *Magn Reson Med* 2010;64:645–52.
- [16] Pregosin PS, Kumar PGA, Fernandez I. Pulsed gradient spin-echo (PGSE) diffusion and H-1, F-19 heteronuclear overhauser spectroscopy (HOESY) NMR methods in

- inorganic and organometallic chemistry: something old and something new. *380 Chem Rev* 2005;105:2977–98. 381
- [17] Cohen Y, Avram L, Frish L. Diffusion NMR spectroscopy in supramolecular and 382 combinatorial chemistry: an old parameter—new insights. *Angew Chem Int Ed* 383 2005;44:520–54. 384
- [18] Canzi G, Mrse AA, Kubial CP. Diffusion-ordered nmr spectroscopy as a reliable 385 alternative to tem for determining the size of gold nanoparticles in organic 386 solutions. *J Phys Chem C* 2011;115:7972–8. 387
- [19] Marega R, Aeoulmoji V, Dinon F, Vaccari L, Giordani S, Bianco A, et al. Diffusion- 388 ordered NMR spectroscopy in the structural characterization of functionalized 389 carbon nanotubes. *J Am Chem Soc* 2009;131:9086–93. 390
- [20] Callaghan PT, Macgowan D, Packer KJ, Zalaya FO. High-resolution q-space imaging 391 in porous structures. *J Magn Reson* 1990;90:177–82. 392
- [21] Callaghan PT, Coy A, Macgowan D, Packer KJ, Zalaya FO. Diffraction-like effects in 393 NMR diffusion studies of fluids in porous solids. *Nature* 1991;351:467–9. 394
- [22] Callaghan PT. Pulsed-gradient spin-echo NMR for planar, cylindrical, and 395 spherical pores under conditions of wall relaxation. *J Magn Reson Ser A* 396 1995;113:53–9. 397
- [23] Shemesh N, zarlsan E, Basser PJ, Cohen Y. Detecting diffusion–diffraction patterns 398 in size distribution phantoms using double-pulsed field gradient NMR: theory and 399 experiments. *J Chem Phys* 2010;132(1–12):034703. 400
- [24] Cotts RM, Hoch MJR, Sun T, Markert JT. Pulsed field gradient stimulated echo 401 methods for improved NMR diffusion measurements in heterogeneous systems. *J* 402 *Magn Reson* 1989;83:252–66. 403
- [25] Zheng G, Price WS. Suppression of background gradients in (B-0 gradient-based) 404 NMR diffusion experiments. *Concepts Magn Reson A* 2007;30:261–77. 405
- [26] Bar-Shir A, Cohen Y. Crossing fibers, diffractions and nonhomogeneous magnetic 406 field: correction of artifacts by bipolar gradient pulses. *Magn Reson Imaging* 407 2008;26:801–8. 408
- [27] Cory DG, Garraway AN. Measurement of translational displacement probabilities 409 by NMR—an indicator of compartmentation. *Magn Reson Med* 1990;14: 410 435–44. 411
- [28] Assaf Y, Cohen Y. Structural information in neuronal tissue as revealed by q-space 412 diffusion NMR spectroscopy of metabolites in bovine optic nerve. *NMR Biomed* 413 1999;12:335–44. 414
- [29] Assaf Y, Cohen Y. Assignment of the water slow-diffusing component in the 415 central nervous system using q-space diffusion MRS: implications for fiber tract 416 imaging. *Magn Reson Med* 2000;43:191–9. 417
- [30] Biton E, Mayk A, Assaf Y, Cohen Y. Structural changes in glutamate cell swelling 418 followed by multiparametric q-space diffusion MR of excised rat spinal cord. *Magn* 419 *Reson Imaging* 2004;22:661–72. 420
- [31] Bar-Shir A, Cohen Y. High b-value q-space diffusion MRS of nerves: structural 421 information and comparison with histological evidence. *NMR Biomed* 2008;21: 422 165–74. 423
- [32] Ong HH, Wright AC, Wehrli SL, Souza A, Schwartz ED, Hwang SN, et al. Indirect 424 measurement of regional axon diameter in excised mouse spinal cord with q- 425 space imaging: simulation and experimental studies. *Neuroimage* 2008;40: 426 1619–32. 427
- [33] Cory DG, Garraway AN, Miller JB. Applications of spin transport as a probe of local 428 geometry. *Polymer Preprints* 1990;3:149–50. 429
- [34] Mitra PP. Multiple wave-vector extension of the NMR pulsed-field-gradient spin- 430 echo diffusion measurement. *Phys Rev B* 1995;51:15074–8. 431
- [35] zarlsan E, Basser PJ. MR diffusion–“diffraction” phenomenon in multipulse-field- 432 gradient experiments. *J Magn Reson* 2007;188:285–94. 433
- [36] Shemesh N, Cohen Y. The effect of experimental parameters on the signal decay in 434 double-PGSE experiments: negative diffractions and enhancement of structural 435 information. *J Magn Reson* 2008;195:153–61. 436
- [37] zarlsan E, Basser PJ. Microscopic anisotropy revealed by NMR double pulsed field 437 gradient experiments with arbitrary timing parameters. *J Chem Phys* 2008;128(1- 438 11):154511. 439
- [38] zarlsan E. Compartment shape anisotropy (CSA) revealed by double pulsed field 440 gradient MR. *J Magn Reson* 2009;199:56–67. 441
- [39] zarlsan E, Shemesh N, Basser PJ. A general framework to quantify the effect of 442 restricted diffusion on the NMR signal with applications to double pulsed field 443 gradient NMR experiments. *J Chem Phys* 2009;130(1–9):104702. 444
- [40] Komlos ME, zarlsan E, Lizak M, Horkay F, Schram V, Shemesh N, et al. Pore 445 diameter mapping using double pulsed-field gradient MRI and its validation using 446 a novel glass capillary array phantom. *J Magn Reson* 2011;208:128–35. 447
- [41] zarlsan E, Komlos ME, Lizak MJ, Horkay F, Basser PJ. Double pulsed field gradient 448 (double-PFG) MR imaging (MRI) as a means to measure the size of plant cells. 449 *Magn Reson Chem* 2011;49:S79–84. 450
- [42] Shemesh N, zarlsan E, Basser PJ, Cohen Y. Measuring small compartmental 451 dimensions with low-q angular double-PGSE NMR: the effect of experimental 452 parameters on signal decay. *J Magn Reson* 2009;198:15–23. 453
- [43] Shemesh N, zarlsan E, Bar-Shir A, Basser PJ, Cohen Y. Observation of restricted 454 diffusion in the presence of a free diffusion compartment: single- and double-PFG 455 experiments. *J Magn Reson* 2009;200:214–25. 456
- [44] Shemesh N, Cohen Y. Probing microscopic architecture of opaque heterogeneous 457 systems using double-pulsed-field-gradient NMR. *J Am Chem Soc* 2011;133: 458 6028–35. 459
- [45] Shemesh N, zarlsan E, Basser PJ, Cohen Y. Accurate noninvasive measurement of 460 cell size and compartment shape anisotropy in yeast cells using double-pulsed 461 field gradient MR. *NMR Biomed* 2012;25:236–46. 462
- [46] Shemesh N, Cohen Y. Overcoming apparent susceptibility-induced anisotropy 463 (aStA) by bipolar double-pulsed-field-gradient NMR. *J Magn Reson* 2011;212: 464 362–9. 465

- 466 [47] Koch MA, Finsterbusch J. Compartment size estimation with double wave-vector 474
467 diffusion-weighted imaging. *Magn Reson Med* 2008;60:90–101. 475
468 [48] Avram L, Assaf Y, Cohen Y. The effect of rotational angle and experimental 476
469 parameters on the diffraction patterns and microstructural information obtained 477
470 from q-space diffusion NMR: implication for diffusion in white matter fibers. 478
471 *J Magn Reson* 2004;169:30–8. 479
472 [49] Cohen Y, Assaf Y. High b-value q-space analyzed diffusion-weighted MRS and MRI 480
473 in neuronal tissues – a technical review. *NMR Biomed* 2002;15:516–42. 481
482 [50] Weber T, Ziener CH, Kampf T, Herold V, Bauer WR, Jakob PM. Measurement of 474
475 apparent cell radii using a multiple wave vector diffusion experiment. *Magn Reson* 476
477 *Med* 2009;61:1001–6. 478
479 [51] Koch MA, Finsterbusch J. Towards compartment size estimation in vivo based on 479
480 double wave vector diffusion weighting. *NMR Biomed* 2011;24:1422–32. 480
481 [52] Shemesh N, Özarslan E, Konlsh, ME, Bassar PJ, Cohen Y. From single-pulsed field 481
482 gradient to double-pulsed field gradient MR: gleaning new microstructural 482
483 information and developing new form of contrast in MRI. 483

UNCORRECTED PROOF

AUTHOR QUERY FORM

 ELSEVIER	Journal: MRI Article Number: 7891	Please e-mail or fax your responses and any corrections to: Elsevier E-mail: corrections.esi@elsevier.spitech.com Fax: +1 619 699 6721
--	--	--

Dear Author,

Please check your proof carefully and mark all corrections at the appropriate place in the proof (e.g., by using on-screen annotation in the PDF file) or compile them in a separate list. Note: if you opt to annotate the file with software other than Adobe Reader then please also highlight the appropriate place in the PDF file. To ensure fast publication of your paper please return your corrections within 48 hours.

For correction or revision of any artwork, please consult <http://www.elsevier.com/artworkinstructions>.

Any queries or remarks that have arisen during the processing of your manuscript are listed below and highlighted by flags in the proof. Click on the 'Q' link to go to the location in the proof.

Location in article	Query / Remark: click on the Q link to go Please insert your reply or correction at the corresponding line in the proof
Q1	Please confirm that given names and surnames have been identified correctly.
Q2	Please check data here.
Q3	Please provide page range here.
Q4	Please provide the complete bibliographic details of this reference. <div style="border: 1px solid black; padding: 5px; display: inline-block;"> Please check this box if you have no corrections to make to the PDF file. <input type="checkbox"/> </div>

Thank you for your assistance.